Article:
Somvanshi, D, Chauhan, D, Perera, AGU et al. (3 more authors) (2018) Analysis of Barrier Parameters on the Extended Threshold Wavelength of Infrared Detectors. IEEE Photonics Technology Letters, 30 (18). pp. 1617-1620. ISSN 1041-1135

https://doi.org/10.1109/LPT.2018.2860631

Analysis of barrier parameters on the extended threshold wavelength of infrared detectors

Divya Somvanshi, Member IEEE, Dilip Chauhan, A. G. Unil Perera, Fellow IEEE, Lianhe Li, L. Chen, and Edmund H. Linfield

Abstract—The threshold wavelength (λ_t) of spectral photoresponse of any semiconductor photodetector is determined by the minimum energy gap ($\Delta = 1.24/\lambda_t$) of the material, or the interfacial energy gap of the heterostructure. It was shown before that the threshold limit can be extended beyond λ_t to obtain an extended threshold wavelength λ_{eff} ($\lambda_{eff} >> \lambda_t$) in detectors with a barrier energy offset (δE_v) and a gradient. Here, in this letter, we analyze the effect of barrier parameters such as δE_v and gradient on the extended threshold wavelength of infrared detectors for the temperature range up to 50 K.

Index Terms— Infrared photodetectors, threshold wavelength, heterojunction

I. INTRODUCTION

In general, the threshold wavelength of spectral photoresponse of any semiconductor detector is determined by the minimum energy gap (Δ) of the material, or the interfacial energy gap of the heterostructure detector [1, 2]. Extension of threshold wavelength beyond the typical threshold limit ($\lambda_t = 1.24/\Delta$) in heterostructure based infrared (IR) photodetectors was reported recently [1]. A heterostructure detector with a graded barrier and a barrier energy offset at T = 5.3 K showed extended threshold wavelength ($\lambda_{eff} = 1.24/\Delta'$, where Δ' is effective activation energy, $\lambda_{eff} >> \lambda_t$) up to 55 μm whereas the λ_t was 3.9 μm [1].

A p-GaAs/$Al_xGa_{1-x}As$ heterostructure consists of an absorber/emitter (p-type GaAs) sandwiched between high energy undoped $Al_xGa_{1-x}As$ injector (graded or flat) barrier and low energy undoped $Al_xGa_{1-x}As$ collector (flat) barrier. The barrier energy difference between these two barriers is referred as the barrier energy offset (δE_v). Upon incident of infrared radiation, photo excited carriers i.e. hot carriers are generated in the injector, absorber and collector. The photo-absorption in the p-GaAs absorber excites hot carriers from the light/heavy hole bands into the split-off band [3], and these excited carriers then escape into the barrier region, typically interact with cold carriers and are collected at the contact region. The basic model to explain the λ_{eff} in IR detectors is based on the hot carrier effects [4-6]. In that kind of IR detectors, for a net flow of hot carriers δE_v is critical and increasing δE_v and the gradient of the injector barrier; will increase the carrier flow. Hot carriers injected from the high energy barrier side interact with cold carriers in the absorber that leads to non-equilibrium carrier distribution to the specific momentum states and elevated carrier temperature in the absorber [5]. The hot carriers evolve towards equilibrium via momentum and energy relaxation, on a femtosecond (fs) or picoseconds (ps) time scale via elastic and inelastic scattering [7, 8]. Carrier–carrier scattering results in coulomb thermalization and allows the carrier distribution to be described by a quasi-Fermi level with carrier temperature (T_c) > lattice temperature (T_L). Finally, the escape of hot carriers from that quasi-Fermi level across the collector barrier when a long wavelength photon is absorbed gives the extended wavelength threshold photoresponse λ_{eff} ($\lambda_{eff} >> \lambda_t$) [6]. However, in conventional heterostructure detectors with $\delta E_v = 0$, spectral photoresponse with designed λ_t have been observed.

Here we discuss the effect of barrier parameters on the extended threshold wavelength of heterostructure detectors up to 50 K.

II. EXPERIMENTAL DETAILS

The three IR p-GaAs/ $Al_xGa_{1-x}As$ heterostructure detectors, SP1001, SP1007 and 15SP3, were grown by molecular beam epitaxy on a semi-insulating GaAs (100) substrate. Each p-GaAs/$Al_xGa_{1-x}As$ IR detector structure consist of three p-type GaAs regions ($p = 1\times10^{19}$ cm^{-3}), i.e. bottom contact, absorber (emitter) and top contact. The active region of each IR detector consists of p-GaAs of 80 nm thickness with the bottom and top contacts have the thicknesses of 80 nm and 400 nm respectively. Detector SP1001 have a flat high energy barrier and low energy flat barrier with barrier energy offset (δE_v) = 0.10 eV. Detector SP1007 have a high energy barrier with graded profile and δE_v = 0.10 eV. Detector 15SP3 have a similar structure as SP1007 except δE_v = 0.19 eV. By varying the Al fractions, the detectors SP1007 and 15SP3 have a graded potential profile and energy offset between the barriers. For comparison, a flat barrier detector LH1002 with δE_v = 0 was also designed with thickness of absorber 18.8 nm and the bottom and top contacts 60 nm respectively. Mesas with an electrically active area of 400×400 μm^2 were fabricated by the conventional photolithography and wet etching, and the contact electrodes were formed by Ti/Pt/Au metallization. By partially etching the top contact layer, an optical window of ~260×260 μm^2 was opened for normal incidence optical illumination of the detector. For photoresponse measurements,

This work was supported, in part, by the U.S. Army Research Office under Grant No. W911 NF-15-1-0018 and, in part, by National Science Foundation (NSF) under Grant No. ECCS-1232184. Funding was also received from the European Community's Seventh Framework Programme (FP7) under Grant Agreement No. 247375 "TOSCA".

D. Chauhan and A. G. U. Perera are at the Department of Physics and Astronomy, Georgia State University, Atlanta, 30303 GA (e-mail: uperera@gsu.edu)

D. Somvanshi was at the Department of Physics and Astronomy, Georgia State University, Atlanta, 30303, USA. She is now at the Department of Electronics and Tele-Communication Engineering, Jadavpur University, Kolkata -700032, India.

Lianhe Li, L. Chen and E. H. Linfield are at the School of Electronic and Electrical Engineering, University of Leeds, Leeds LS2 9JT, UK.

samples were mounted in a liquid helium Dewar and a black body source with peak intensity of 2.8 mW/cm^2 is used to measure the photoresponse spectra (Perkin–Elmer system 2000 Fourier transform infrared (FTIR) spectrometer) of all the detectors under study. The bias voltage in the photoresponse measurement was measured using Keithley 1600 Electrometer, and the negative bias refers to the positive voltage connected to the bottom contact, with the top contact grounded and vice versa. A bolometer with known sensitivity was used for background measurements and calibrating the responsivity. The comparison of Al fraction, thicknesses and $\boldsymbol{\delta}E_v$ for all detectors used in this study are listed in Table. I.

TABLE I
TABLE.1 STRUCTURAL PARAMETERS FOR ALL IR DETECTORS: ALUMINUM MOLE FRACTION, BARRIER ENERGY OFFSET ($\boldsymbol{\delta}E_v$) AND THICKNESSES

Sample	Al mole fraction				$\boldsymbol{\delta}E_v$	Thickness (nm)		
	x_1	x_2	x_3	x_4	(eV)	w_1	w_2	w_3
SP1001	0.75	0.75	0.57	0.57	0.10	80	80	400
SP1007	0.45	0.75	0.57	0.57	0.10	80	80	400
15SP3	0.45	0.75	0.39	0.39	0.19	80	80	400
LH1002	0.57	0.57	0.57	0.57	0	60	18.8	60

Fig. 1(a), (b) and (c) shows unbiased valence band (VB) diagram of samples SP1001, SP1007, 15SP3 and LH1002 under dark condition. In all the detectors, the bottom contact (BC), the absorber (p-GaAs) and top contact (TC) are highly doped. The Fermi level (E_f) in the p-doped GaAs absorber lies in the light hole (LH)/heavy hole (HH) band, with the spin-orbit split-off (SO) band separated by 340 meV from the LH/HH band near k = 0 as shown in Fig. 1(d). The energy difference between the Fermi level and the top of the valance band edge is denoted as the potential energy barrier (Δ). The carrier transport over Δ takes place via thermionic emission (since the barriers are thick enough, tunneling can be ignored) [9]. The dark current of a heterostructure detector is described by a 3D carrier drift

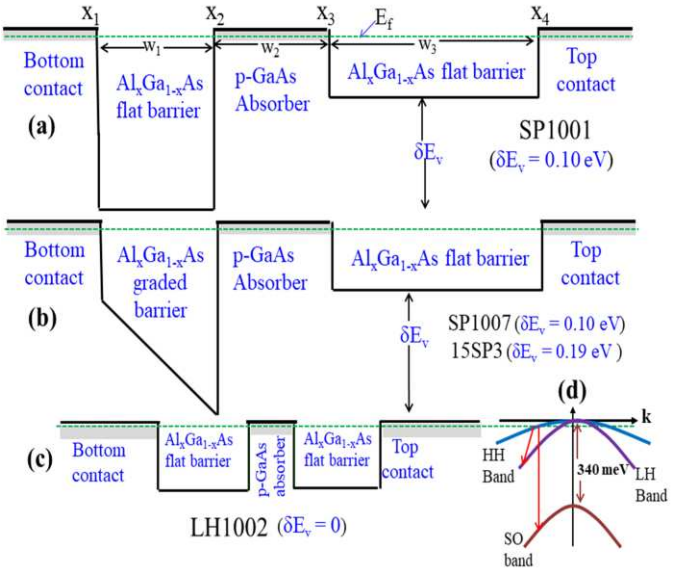

Fig.1. Unbiased schematic VB diagram of (a) Detector SP1001 with p-GaAs absorber, flat high energy $Al_xGa_{1-x}As$ barrier, flat low energy $Al_xGa_{1-x}As$ barrier and $\boldsymbol{\delta}E_v$ = 0.10 eV (b) detector SP1007 have similar structure as SP1001 except graded barrier with $\boldsymbol{\delta}E_v$ = 0.10 eV and detector 15SP3 have similar structure as SP1007, except $\boldsymbol{\delta}E_v$ = 0.19 eV(c) LH1002 consists of a p-GaAs absorber and bottom contact and top contact of $Al_xGa_{1-x}As$ with $\boldsymbol{\delta}E_v$ = 0. (d) A schematic of the valence band of the p-GaAs absorber shows hole transition from LH/HH band, to SO band which is separated from LH/HH band by 340 meV.

model [9, 10], and for a given value of the electric field, the $I_{dark} \propto T^{3/2} \exp\left(-\Delta/kT\right)$ and $\Delta = 1.24/\boldsymbol{\lambda}_t$. Therefore the dark current of all the detectors is determined by the designed value of Δ and remains unaffected.

Upon incidence of light from an external optical source, holes transitions taking place either between different bands (intervalence-band absorption) or within the same band (free-carrier absorption)[3] Holes surmounting the barrier are 'hot' because of their excess energies relative to the valance band-edge of the absorber. In SP1001 and SP1007, 15SP3 [fig. 1 (a) and fig. 1(b)] a net flow of hot holes observed owing to the difference in barrier heights, ΔE_v even at zero bias and an extended threshold wavelength $\boldsymbol{\lambda}_{eff} = 1.24/\Delta'$ where $\boldsymbol{\lambda}_{eff} >> \boldsymbol{\lambda}_t$ is observed. For LH1002 as shown in Fig. 1(c), no net flow of hot holes observed due to the symmetry of the detector. However upon application of bias, $\boldsymbol{\lambda}_t = 1.24/\Delta$ observed with slight variation in $\boldsymbol{\lambda}_t$ with increasing bias due to image force induced barrier lowering effect [10]. The interaction of hot holes and cold holes (holes which are already present in p-GaAs absorber due to doping) in the absorber leads to mechanism responsible for extended threshold wavelength in detectors SP1001, SP1007 and 15SP3 as already mentioned in details in Ref [6].

In general, by increasing thickness of p-GaAs absorber, the absorption in material increases which can change the position of the peak responsivity and spectral width of photoresponse up to a certain limit [9, 11]. Since, the $Al_xGa_{1-x}As$ barriers are undoped and will not produce any photo carriers; therefore the thickness differences don't have any contribution in the extension of threshold wavelength beyond $\boldsymbol{\lambda}_t$. In this work, samples with different thicknesses of barrier and absorber have compared; thus, all the photoresponse spectra have analyzed at the close value of the electric field.

III. RESULTS AND DISCUSSIONS

The heterostructure detectors operate based on the internal photoemission process (IPE) process where carriers are photoexcited and escape from one material to another by passing through an absorber/barrier interface [9, 12]. The photoemission efficiency is proportional to $(\varepsilon - \Delta)$, where $\boldsymbol{\varepsilon}$ is the energy of the photo-excited holes and Δ is the potential energy barrier at the interface.

The quantum yield defined as the number of collected photo carriers per incident photon can be described by the following expression

$$Y(h\nu) = Y_0(kT) + C_0 \int_{\Delta}^{\infty} \rho(\varepsilon, h\nu) f(\varepsilon, h\nu) P(\varepsilon, \Delta) d\varepsilon \qquad (1)$$

which takes into account two essential processes during IPE, photo excitation in the absorber [described by an energy distribution function $\rho(\varepsilon, h\nu)$] and the transmission of carriers over a barrier [describe by probability distribution function $P(\varepsilon, \Delta)$]. In this work, the Δ of spectral photoresponse is determined by temperature-dependent internal photoemission spectroscopy (TDIPS) method [13], where the quantum yield is proportional to the multiplication of spectral responsivity and photon energy. Thus to obtain Δ, the quantum yield (x-axis) plotted as a function of photon energy (y-axis) and fittings to this spectrum were carried out in the near-threshold regime by using Eq. (1) where Y_0, C_0, and Δ are regarded as fitting parameters.

A. Heterostructure detectors with and without barrier energy offset

The photoresponse spectra of detectors LH1002 ($\delta E_v = 0$) and SP1001 ($\delta E_v = 0.10$ eV) are compared at 5.3 K and E ~ -10.41 kV/cm as shown in Fig. 2(a). At T = 5.3 K, SP1001 have detectable λ_{eff} ~36 μm (due to noise at the threshold end) which is much longer than the designed λ_t ~3.1 μm of SP1001. However, the photoresponse spectra of LH1002 shows threshold wavelength of 4.3 μm which is close to the designed λ_t = 4.1 μm. Therefore, it is clear that extended threshold wavelength observed only for SP1001 at 5.3 K.

Now, the photoresponse spectra of LH1002 and SP1001 are compared at 50 K and E ~ -20.83 kV/cm as shown in Fig. 2 (b), inset of fig. 2(b) shows the TDIPS fitting results for LH1002 and SP1001 at 50 K. A close value of threshold wavelength of 4.2 μm for LH1002 and 4.1 μm for SP1001 is observed at 50 K. By comparison of photoresponse spectra of both samples at 5.3 K and 50 K, it is observed that as the temperature goes up from 5.3 K to 50 K, the λ_{eff} comes down closer to the λ_t for SP1001 whereas for LH1002, not much change in λ_t is observed as temperature changes from 5.3 K to 50 K. This observation suggests that the δE_v is critical to obtain λ_{eff} (>>λ_t) in IR detectors for a given value of temperature. However, it may also be noted here that the observation of λ_{eff} is also depended on temperature. In this view, the dependence of λ_{eff} on the temperature up to 90 K was already reported as mentioned in Ref [12].

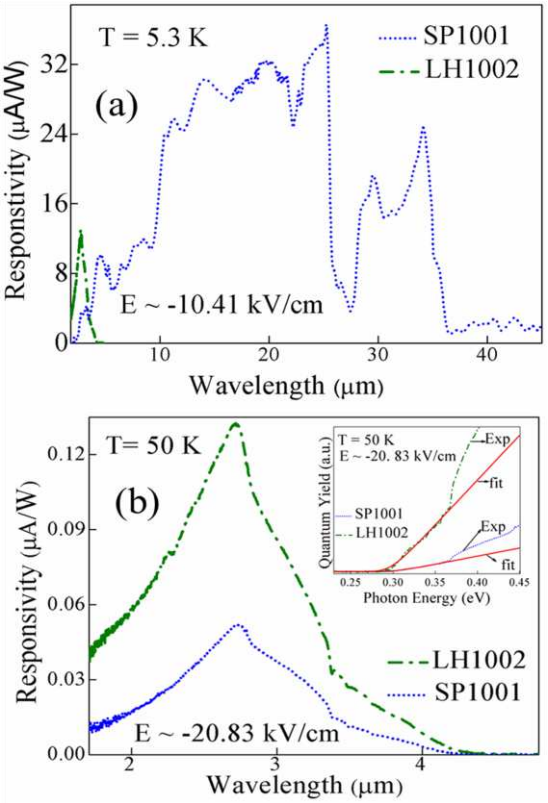

Fig. 2. Photoresponse spectra of SP1001 and LH1002 (a) at 5.3 K, SP1001 shows λ_{eff} ~ 36 μm whereas LH1002 which shows λ_{eff} ~ 4.3 μm close to λ_t, (b) at 50 K, SP1001and LH1002 shows λ_{eff} ~ λ_t; inset shows TDIPS fitting of LH1002 and SP1001 that confirm that the threshold wavelength remains almost same, solid (red) and dashed lines represent TDIPS fitting and experimental curves.

B. Heterostructure detectors (similar barrier energy offset) with flat and graded barrier

The photoresponse spectra of two detectors with a similar value of δE_v but one with a flat injector barrier (SP1001) and other with a graded injector barrier (SP1007) have compared in Fig. 3(a) at 50 K and E ~ -20.83 kV/cm. From the VB diagram of Fig. 1(a) and (b), it is observed that due to the graded high energy barrier, hot holes of varying energy can overcome the injector/absorber barrier. However, with flat high energy barrier, hot holes with energy corresponding to only higher potential barrier can overcome the barrier. Thus, it is expected that efficiency of the hot - cold hole interaction in the absorber decreases for SP1001 which could be the prime mechanism of extended threshold wavelength in SP1001 and SP1007 [6]. Therefore, photoresponse with clear λ_{eff} observed in SP1007 even at a small value of the electric field as compared to SP1001.

The photoresponse spectra of SP1007 shows a clear λ_{eff} = 8.9 μm, however the designed λ_t = 3.1 μm. However, SP1001 shows λ_{eff} = 4.1 μm very close to the designed λ_t = 3.1 μm. The TDIPS fitting for SP1007 are shown in the inset of Fig. 3(a) where for SP1001 is already in the inset of Fig. 2(b). Thus, a clear extension observed in threshold wavelength for SP1007 at 50 K. This implies that by changing the high energy barrier from flat to graded (without changing the δE_v), a clear λ_{eff} can be observed at 50 K. It may be noted here, since the responsivity of SP1001 data is order of ~0.05 μA/W (see Fig. 2 b), and SP1007 is of ~108 μA/W and for comparison in single Fig, we have multiplied responsivity of SP1001 by ×120 to just show visibility of data in one spectra.

To further analyze the effect of the gradient on λ_{eff}, the

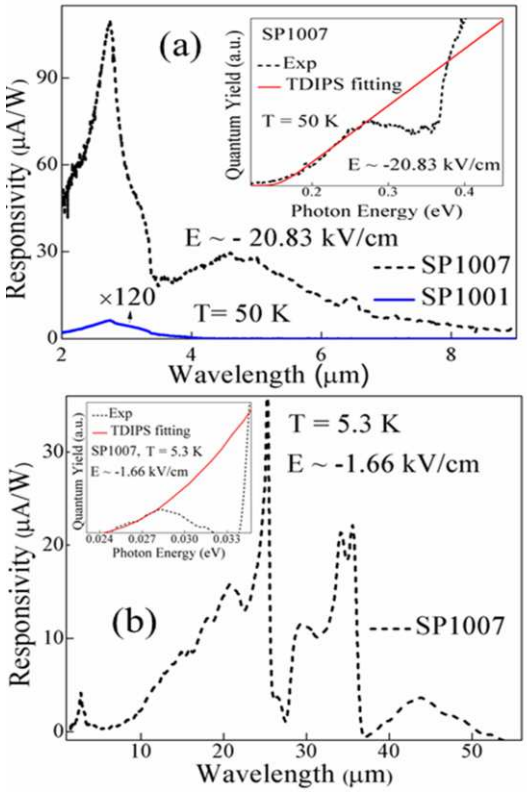

Fig. 3 (a) Photoresponse spectra of SP1001 and SP1007, as barrier changes from flat to graded, the λ_{eff} increases from 4.1 μm to 8.9 μm, inset shows TDIPS fitting for photoresponse spectra of SP1007 at 50 K, solid and dashed lines represent fitted and experimental curves (b) Photoresponse spectra of SP1007 at 5.3 K, a clear λ_{eff} = 55 μm is observed as compare to SP1001 of λ_{eff} ~ 36 μm at 5.3 K (see the Fig. 2(a)), inset shows TDIPS fitting for SP1007.

photoresponse spectrum of SP1007 is shown in Fig. 3(b) at T = 5.3 K with inset shows TDIPS fitting of the data. The data is recorded at the E ~ -1.66 kV/cm, for SP1007 the λ_{eff} started at a very small electric field and with the application of an electric field it shows a very slight increase in λ_{eff}. Thus for SP1007, a clear λ_{eff} = 55 μm at E ~ -1.66 kV/cm observed; whereas in SP1001 an extended photoresponse is clearly observable, but λ_{eff} is detectable only up to ~36 μm (as already shown in Fig. 2(a)) even at higher E ~ -10.41 kV/cm. This comparison shows that although extended photoresponse is observed for both detectors, i.e., SP1001 and SP1007, the clear λ_{eff} only observed for SP1007 at 5.3 K. Therefore, the graded barrier across injector barrier along with barrier energy offset is needed for observation of clear λ_{eff} at a higher temperature.

C. Heterostructure detectors (similar graded barrier) with different barrier energy offset.

The photoresponse spectra of two detectors having similar device structure except two different barrier energy offsets, i.e., 15SP3 (δE_v = 0.19 eV) and SP1007 (δE_v = 0.10 eV) are compared at 50 K and E ~ -20.83 kV/cm as shown in Fig. 4(a). The TDIPS fitting for 15SP3 is shown in Fig. 4(b) and for SP1007 it is already given in the inset of Fig. 3 (a). For 15SP3 the λ_{eff} = 13.7 μm whereas for SP1007, λ_{eff} = 8.9 μm is observed, however the designed λ_t is 3.1 μm for both detectors. Therefore, it is observed by increasing δE_v from 0.10 eV to 0.19 eV (for the similar graded barrier), the λ_{eff} increases from 8.9 μm to 13.7 μm. This suggests that the value of λ_{eff} can be increased, for a given graded injector barrier by optimizing value of δE_v. The possible reason is, by varying δE_v the number of hot holes injected into the absorber and escaping across the collector barrier can be controlled which consequently control the λ_{eff}. Therefore, by using a higher value of δE_v a much longer λ_{eff} can be obtained for a given temperature.

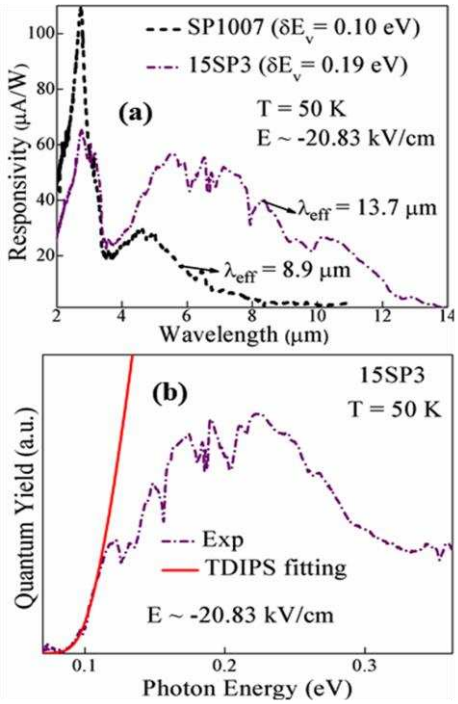

Fig.4. (a) Photoresponse spectra of SP1007 and 15SP3 at 50 K, as δE_v increases from 0.10 eV to 0.19 eV the λ_{eff} increases from 8.9 μm to 13.7 μm. (b) TDIPS fitting for the photoresponse of 15SP3 to obtain the Δ of the spectral photoresponse at 50 K, solid and dotted lines represent fitted and experimental curves, respectively.

IV. Conclusion

In conclusion, the analysis of barrier design parameters on the extended threshold photoresponse of IR detectors has discussed in details up to 50 K. It is observed the δE_v is critical to obtain λ_{eff} (>>λ_t) in IR detectors at 5.3 K, however the gradient is needed to obtain λ_{eff} at 50 K. A conventional detector (LH1002), shows $\lambda_t \sim \lambda_{eff}$ over operating temperature from 5.3 K and 50 K whereas the flat injector barrier and barrier energy offset detector (SP1001) shows λ_{eff} ~36 μm at 5.3 K and 4.1 μm at 50 K. When the high energy injector barrier changes from flat (SP1001) to graded (SP1007), the λ_{eff} increases from 4.1 μm to 8.9 μm at 50 K. For a given graded injector barrier, as δE_v increases from 0.10 eV to 0.19 eV, the λ_{eff} increases from 8.9 μm to 13.7 μm. The results of this study indicate that by optimization of δE_v and the gradient, IR detectors with λ_{eff} (>>λ_t) can be designed to operate over a wide range of temperature for practical device applications.

References

[1] Y.-F. Lao, A. G. U. Perera, L. H. Li, S. P. Khanna, E. H. Linfield, and H. C. Liu, "Tunable hot-carrier photodetection beyond the bandgap spectral limit," Nat. Photon., vol. 8, pp. 412-418, 2014.

[2] D. Chauhan, A. G. U. Perera, L. Li, L. Chen, S. P. Khanna, and E. H. Linfield, "Extended wavelength infrared photodetectors," Opt. Eng., vol. 56, pp. 091605-091605, 2017.

[3] Y. F. Lao, P. K. D. D. P. Pitigala, A. G. U. Perera, H. C. Liu, M. Buchanan, Z. R. Wasilewski, et al., "Light-hole and heavy-hole transitions for high-temperature long-wavelength infrared detection," Appl. Phys. Lett., vol. 97, pp. 091104, 2010.

[4] J. Shah, "Hot carriers in quasi-2-D polar semiconductors," IEEE J Quantum Electron., vol. 22, pp. 1728-1743, 1986.

[5] M. L. Brongersma, N. J. Halas, and P. Nordlander, "Plasmon-induced hot carrier science and technology," Nat. Nano., vol. 10, pp. 25-34, 2015.

[6] D. Somvanshi, D. Chauhan, Y. F. Lao, A. G. U. Perera, L. Li, S. P. Khanna, et al., "Analysis of Extended Threshold Wavelength Photoresponse in Nonsymmetrical p-GaAs/AlGaAs Heterostructure Photodetectors," IEEE J. Sel. Top. Quantum Electron., vol. 24, pp. 1-7, 2018.

[7] D. J. Erskine, A. J. Taylor, and C. L. Tang, "Femtosecond studies of intraband relaxation in GaAs, AlGaAs, and GaAs/AlGaAs multiple quantum well structures," Appl. Phys. Lett., vol. 45, pp. 54-56, 1984.

[8] J. Shah, A. Pinczuk, A. C. Gossard, and W. Wiegmann, "Energy-Loss Rates for Hot Electrons and Holes in GaAs Quantum Wells," Phys. Rev. Lett., vol. 54, pp. 2045-2048, 1985.

[9] D. G. Esaev, M. B. M. Rinzan, S. G. Matsik, and A. G. U. Perera, "Design and optimization of GaAs⁄AlGaAs heterojunction infrared detectors," J. Appl. Phys, vol. 96, pp. 4588-4597, 2004.

[10] D. Chauhan, A. G. U. Perera, L. H. Li, L. Chen, and E. H. Linfield, "Dark current and photoresponse characteristics of extended wavelength infrared photodetectors," J. Appl. Phys, vol. 122, pp. 024501, 2017.

[11] S. G. Matsik, R. C. Jayasinghe, A. B. Weerasekara, A. G. U. Perera, E. H. Linfield, S. P. Khanna, et al., "Effect of emitter thickness on the spectral shape of heterojunction interfacial workfunction internal photoemission detectors," J. Appl. Phys., vol. 106, pp. 014509, 2009.

[12] Y.-F. Lao, A. G. U. Perera, L. Li, S. P. Khanna, E. H. Linfield, Y. Zhang, et al., "Mid-infrared photodetectors operating over an extended wavelength range up to 90 K," Opt. lett., vol. 41, pp. 285-288, 2016.

[13] Y.-F. Lao and A. G. U. Perera, "Temperature-dependent internal photoemission probe for band parameters," Phys. Rev. B, vol. 86, p. 195315, 2012.